

Impact of Data Quality on Renewable Energy Potential Estimations

Stanley Risch^{a,*}, Rachel Maier^a, Junsong Du^b, Noah Pflugradt^a, Peter Stenzel^c, Leander Kotzur^a and Detlef Stolten^{a,d}

^aInstitute of Energy and Climate Research - Techno-economic Systems Analysis (IEK-3), Forschungszentrum Jülich GmbH, Wilhelm-Johnen-Straße, 52428 Jülich, Germany

^bRWTH Aachen University, E.ON Energy Research Center, Institute for Energy Efficient Buildings and Indoor Climate, Mathieustraße 10, Aachen, 52074, Germany

^cTH Köln, Cologne Institute for Renewable Energy (CIRE), Betzdorfer Straße 2, Köln, 50679, Germany

^dRWTH Aachen University, c/o Institute of Energy and Climate Research - Techno-economic Systems Analysis (IEK-3), Forschungszentrum Jülich GmbH, Wilhelm-Johnen-Straße, Jülich, 52428, Germany

ARTICLE INFO

Keywords:

Solar-photovoltaics
Potential analysis
Data quality
3D building models
Energy system modeling

ABSTRACT

Potential analyses identify possible locations for renewable energy installations, such as wind turbines and photovoltaic arrays. The results of previous potential studies, however, are not consistent due to different assumptions, methods, and datasets. In this study, we compare commonly used land use data sources with regard to area and position. Using Corine Land Cover leads to an overestimation of the potential areas in a typical wind potential analysis by a factor of 4.6 and 5.2 in comparison to Basis-DLM and Open Street Map, respectively. Furthermore, we develop scenarios for onshore wind, offshore wind, and open-field photovoltaic potential estimations based on land eligibility analyses and calculate rooftop photovoltaic potential using 3D building data. The potential capacities and possible locations are published for all administrative levels in Germany in the freely accessible database **trep-db**,¹ for example, to be incorporated into energy system models. The investigations are validated using high-resolution regional potential analyses and benchmarked against other studies in the literature. Findings from the literature, which can be used by legislators to design regulation, are rarely comparable and consistent due to differences in the datasets used.

1. Introduction

In 2015, the Paris Climate Agreement [1] was signed by 195 countries with the aim of limiting global temperature increases to below 2 °C above pre-industrial levels. Germany strengthened its ambitions to combat climate change in the Climate Protection Act of 2021 [2] by setting the goal of climate-neutrality in 2045. To achieve this target, the capacity of renewable energy technologies must be greatly increased [3]. However, the specific land requirement of renewable energy technologies as photovoltaic (PV) systems or wind turbines exceeds those of conventional power plants, and therefore larger areas will be needed for the future energy supply. The eligibility and availability of construction areas constitute a limiting factor and determine the region-specific potentials of renewable energy sources.

Energy system models and corresponding studies can support the planning process of future energy systems with high shares of renewable energy. However, the set potentials or renewable expansion goals significantly differ in national energy system studies (see [3, 4, 5, 6, 7, 8, 9]) and often information about methods, data sources, or assumptions is lacking. As energy system analyses can have different regional scopes and levels, internally-consistent potential data on different geographical levels is needed.

Regionalized potentials are estimated with potential analyses, which are performed sequentially: First, eligible ar-

reas for the construction of renewable power installations are determined. Then on the basis of these areas, the potential capacity and energy generation can be estimated. The definition of eligible areas therefore plays a crucial role in the estimation of potentials. Depending on the technology, the calculation of eligible areas can be performed by means of statistical formulas, with building models, or with land eligibility analyses. For technologies requiring 'open space', such as open-field PV and wind, the latter methodology is utilized, which requires geospatial datasets. The results of the eligible areas and the potential capacity are therefore influenced by these datasets; however, the impact has not yet been evaluated [10]. The comparability of studies using different datasets is therefore unknown.

The following analyses the impact of commonly used datasets on land eligibility analyses and presents scenarios for onshore, offshore wind, open-field PV, and rooftop PV potentials in Germany. The structure of the paper is twofold: In the first part (Section 2), the potential analyses on open spaces for open-field PV and offshore and onshore wind are presented. These are based on land eligibility analyses (Section 2.1) using geospatial datasets. We first evaluate land use datasets in the context of potential analyses in Section 2.2, which closes a gap in the literature and also underlines the quality of the following potential analyses. Then, we describe the state of the art and methodology before presenting the results and discuss these for the following technologies: onshore wind (Section 2.3), offshore wind (Section 2.4), and open-field PV (Section 2.5). In the second part of the paper, we present the potential analysis for rooftop PV in Section 3. Thereby, for the first time, 3D building data is used to esti-

*Corresponding author

Email address: s.risch@fz-juelich.de (S. Risch)

ORCID(s): 0000-0002-7188-155X (S. Risch)

¹Tool for Renewable Energy Potentials - Database
(doi: 10.5281/zenodo.6414018)

mate the potential for Germany. For the considered technologies, we benchmark the results against other potential studies to provide insights into the impact of data sources, exclusion criteria and methodologies. The results of our potential analyses are published in the open database **trep-db**, with utility, for instance, for energy system modelers. The area and capacity potentials of high quality and resolution are provided for several scenarios per technology, and for the administrative levels spanning the municipality to national levels in Germany.

2. Renewable energy potentials on open spaces

The following chapter presents the potential analyses for renewable energy technologies that require open space. First, the general methodology and evaluation of the input data for land eligibility analyses is presented in Section 2.1 and 2.2, respectively. Afterwards, potential analyses are performed for onshore wind (Section 2.3), offshore wind (Section 2.4), and open-field PV (Section 2.5).

2.1. Land eligibility analysis

The construction of renewable power generation sites requires eligible land. Therefore, land eligibility analyses based on geospatial data are performed as the first step of open space potential analyses. Geospatial data is used to consider areas eligible, e.g., bare land, or to extract information to identify ineligible areas due to criteria such as physical constraints, such as steep slopes, or regulatory constraints, such as national parks. Aside from considering areas ineligible, a setback around these areas may also not be usable depending on the exclusion criteria. This can be achieved by adding a buffer around identified land use categories. For instance, the construction of wind turbines is not only ineligible for land use categories such as settlements or streets but also within a certain distance around these areas. To perform the land eligibility analysis, the open source tool *GLAES* [11] was applied, which performs the necessary operations using geospatial datasets to determine eligible areas for renewable energy sites. We chose a resolution of 10 m×10 m in the land eligibility analyses to ensure the representation of detailed features for the high-resolution potentials. However, as the chosen datasets have a significant impact on the results of the land eligibility analysis, they are analyzed in the following section.

2.2. Evaluation of land use datasets

To identify geographical features, land eligibility analyses require geospatial datasets that describe land characteristics, e.g., land use, elevation, and water depths. The quality and resolution of the feature representation in the dataset therefore has an impact on the land eligibility analysis. For instance, missing represented urban areas in a settlement dataset can underestimate excluded areas within the potential analyses or a coarse resolution can either under- or overestimate areas depending on its classification. However, even though the datasets influence potential analyses,

McKenna et al. [10] state that the impact of employing different data sources has not yet been evaluated.

In the present section, the first comparison and evaluation of the following four land use datasets for potential analyses is performed for the regional scope of Germany:

- Basis-DLM [12]: Official German dataset with a high positional accuracy (between ± 3 and ± 15 m depending on the feature)
- Corine Land Cover (CLC) [13]: Land cover raster dataset with 100 m×100 m resolution
- Open Street Map (OSM) [14]: User based land cover vector dataset
- World Database on Protected Areas (WDPA) [15]: Vector dataset with information on protected areas

According to McKenna et al. [10], the datasets CLC, OSM, and WDPA are commonly used global and continental ones for potential analyses.

Two parameters are used to compare the covered area using dataset $A(\text{dataset})$ for different features. The first parameter is the Normalized Total Area (NTA) (Equation 1): It describes the covered area by a dataset compared to the maximum area covered by any other dataset capturing the feature:

$$NTA(\text{dataset}_i) = \frac{A(\text{dataset}_i)}{\max_j(A(\text{dataset}_j))} \quad (1)$$

The second parameter is the Intersection over Union (IoU) of two datasets (Equation 2): It describes the area identified by both datasets divided by the area identified when combining the two. An Intersection over Union of 100% describes that identified areas of two datasets as equal:

$$IoU(\text{dataset}_{(i,j)}) = \frac{A(\text{dataset}_i) \cap A(\text{dataset}_j)}{A(\text{dataset}_i) \cup A(\text{dataset}_j)} \quad (2)$$

The calculation of the parameters is performed with additional standard setback distances for wind potential analyses (see the supplementary material). Furthermore, a rasterized representation of the datasets with the corresponding setback distance and a resolution of 10 m×10 m is used.

Figure 1 shows the results for the Normalized Total Area and the Intersection over Union for the analyzed land use categories. The definition of the filter used to identify the respective features in each dataset can be found in the supplementary information. It must be stated that the WDPA only provides information on protected areas, in which its results are only comparable for these. Furthermore, the CLC does not include all presented categories, such as features with narrow widths like roads or power lines.

For the typical wind potential analysis, OSM and Basis-DLM identify the largest area and share the highest Intersection over Union for most categories. For categories of larger sizes, i.e., farmland, forests, mining, and grassland, the CLC

Impact of Data Quality on Renewable Energy Potential Estimations

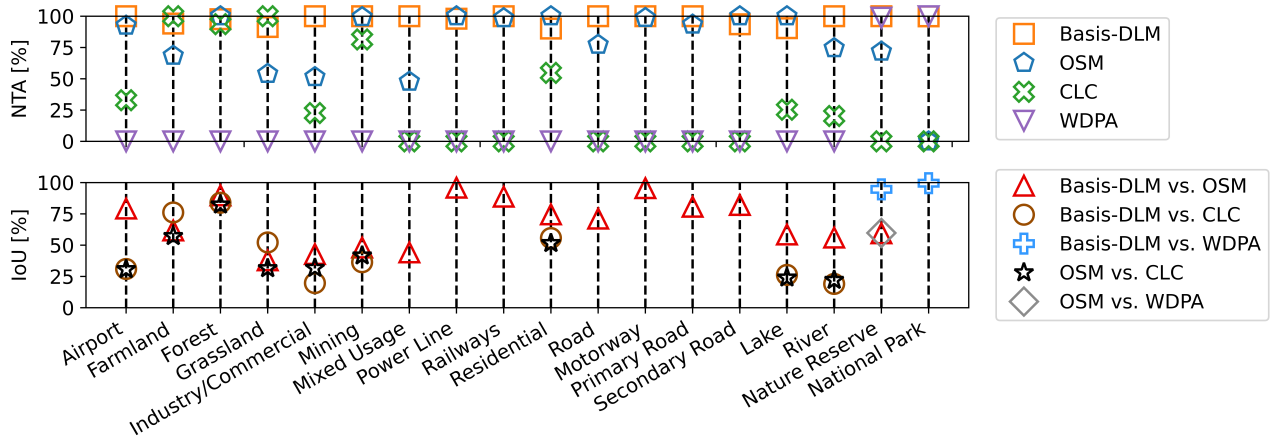


Figure 1: Comparison of the Normalized Total Area (NTA) (upper plot) and Intersection over Union (IoU) (lower plot) per category for the covered area with additional setback distances of a wind potential analysis for different data sources.

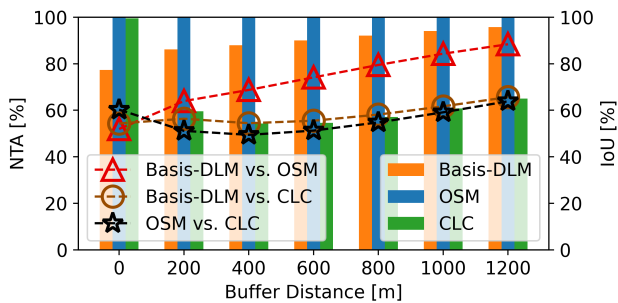


Figure 2: Intersection over Union (bars) and Normalized Total Area (markers) for the residential category for a variation of the setback distance.

classifies a similar buffered area as Basis-DLM. Nevertheless, the Intersection over Unions are only high (above 70%) for the categories of farmland and forests, which means that the identified areas vary largely in position for the categories of mining and grassland. In the nature protection categories ('Nature Reserve', 'National Park'), WDPA and Basis-DLM identify almost identical areas, recognizable through Intersection over Unions near 100%. The OSM-identified nature reserves, on the other hand, show significant deviations from the Basis-DLM and WDPA, whereas national parks cannot be identified with the OSM.

McKenna et al. [10] and Masurowski et al. [16] state that the land use category settlements (often synonymously used with residential land use in land eligibility analyses) highly influences the potential analysis in Germany, which is why the category is further analyzed. For a typical setback distance of 1000 m in Figure 1, the OSM covers the largest area, followed by the Basis-DLM. Figure 2 shows how the Normalized Total Area and Intersection over Union of the residential category behaves when varying the setback distance. Without any buffer, the OSM covers the largest area, closely followed by the CLC. With increasing setback distances, the Normalized Total Area of the CLC first drops

rapidly, whereas the Normalized Total Areas of the Basis-DLM and OSM converge. This indicates that the Basis-DLM and OSM classify more, but smaller settlements in comparison to the CLC. With increasing setback distances of above 600 m, the Normalized Total Area of the CLC increases again, as the buffered areas around smaller features identified by the Basis-DLM and OSM exhibit increasing overlaps. The similarity of the Basis-DLM and OSM is also shown by their Intersection over Union, which increases over the buffer distance of up to 88%. The described behavior of CLC in the residential category, on the other hand, indicates that the representation of smaller detached settlements is missing, whereas larger settlements are covered to a coarser extent. This can be explained by the relatively coarse resolution of 100 m×100 m of the dataset and the minimum mapping unit of 25 ha.

Using CLC to classify residential areas can lead to an underestimation of excluded areas and therefore an overestimation of potential areas, especially for typical setback distances for wind potential analyses of between 600 and 1000 m. Furthermore, CLC cannot represent categories with small size features or widths due to its minimal mapping unit. Therefore, the usage of CLC for potential analyses is not recommended.

The similarity of OSM and Basis-DLM can be seen for multiple categories, e.g., power lines, motorways, in which the Normalized Total Areas and Intersection over Unions are near 100%. For these categories, the use of both datasets is justified.

Figure 3 shows the results of a land eligibility analysis with the setback distances of a typical wind potential analysis (see the supplementary material) for Basis-DLM, OSM, and CLC. When all three of the datasets include the feature, the corresponding dataset is used; otherwise, a default dataset is applied for the exclusion. In particular, the use of the CLC for land eligibility analyses leads to significantly different results. The resulting total potential area using the CLC is roughly 80% higher compared to the OSM and Basis-

DLM. However, the analyses using Basis-DLM and OSM, even though resulting in similar total areas, have discrepancies locating the areas, which is indicated by an Intersection over Union of 64%.

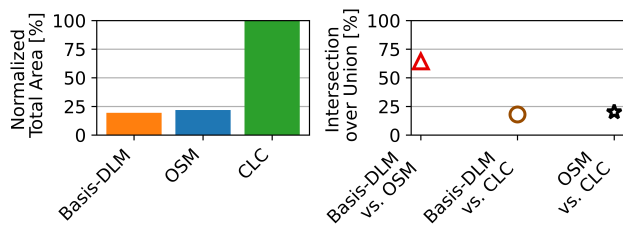


Figure 3: Normalized Total Area and Intersection over Union for the resulting potential areas of a typical wind analysis using different datasets.

In summary, the presented analysis highlights the discrepancy of land use declaration by different datasets, by which the results of potential analyses using different datasets are hardly comparable. Furthermore, the analysis reveals the large sensitivity of land eligibility results regarding the chosen datasets and the importance of data with a high resolution and high positional accuracy for potential analyses.

For the scenarios outlined in this paper and the enclosed database **trep-db**, WDPA is used for the nature protection categories and Basis-DLM for most land use categories in the land eligibility analyses. Further datasets are employed for other individual categories (e.g., water protection areas), but are not considered in this data analysis due to the lack of comparability to other datasets. Basis-DLM was selected due to the exhibited characteristics and is preferred over OSM due to its official character, high positional accuracy, detailed documentation, and the categories covered. Furthermore, for the wind potential analysis, the residential areas are split into inner and outer areas (see Section 2.3.2), which is not possible by the sole use of OSM.

2.3. Onshore wind potential

2.3.1. Literature

Onshore wind analyses are generally performed with a greenfield approach (see, e.g., [17, 18, 19, 20, 21, 22, 23, 24, 25, 26, 4]). Only Masurowski et al. [16] proceed differently: First, initially available areas (pre-selected areas), among others grassland and arable land, are selected and then further exclusion criteria are applied. For the considered studies, apart from the varying approach, the most influential differences correspond to the exclusion definitions, i.e., the used criteria and setback distances, the used data sources (cf. Section 2.2), and the capacity estimations.

All of the cited studies pertain to residential areas. Nevertheless, the setback distances and the data sources vary significantly. Tröndle et al. [18] use the European Settlement Map [27] to identify built-up areas and exclude them without a buffer, whereas Peters et al. [20] and LANUV [21] differentiate the setback distance between inner (1000 m) and outer areas (750, 720 m) for their analysis based on Basis-

DLM, and Amme et al. [22] use OSM [14] to identify residential areas and apply varying setback distances (400 to 1000 m). Masurowski et al. [16] specify 1000 m for housing areas but vary the setback distance in their scenarios, without stating a data source. Others use CLC [13] to exclude settlements with 800 m [23, 28] to 1000 m [29]. Ryberg et al. [23] additionally exclude urban areas from EuroStat Urban [30] with 1200 m setback. Lütkehus et al. [24] exclude residential areas with 600 m based on DLM250 [31]. Moreover, area-based residential, settlement, and urban exclusions of individual residential buildings are specified in two regional potential analyses [21, 25] and [4].

Another frequently discussed topic is the construction of wind turbines in forests. The missing consensus in legislation of the federal states can also be observed in the literature, i.e., Thuringia generally forbids the use of forests for wind turbines, whereas in other federal states, construction of these in forests is ongoing [32]. Ruiz et al. [17] exclude forests in the land eligibility analysis, whereas others [18, 23] allow for construction in forests. Other studies treat forests in a differentiated manner. Coniferous forests in densely-wooded municipalities are cited in the LANUV report [21]. Amme et al. [22] and Peters et al. [20] consider scenarios that include and exclude forests. Meanwhile, Ebner et al. [19] exclude forests in one scenario and allow the construction in 10% for another. Wiehe et al. [26] successively reduce the usable parts of forests in their more restrictive scenarios. Lütkehus et al. [24] exclude forests in federal states with less than 15% forest shares. Furthermore, selective exclusions are performed based on the function of the forest.

Inconsistencies can also be seen for protected landscapes, which are a highly influential exclusion (28% of Germany's area [15]). Several studies [20, 22, 26, 24] regard protected landscapes differently between their scenarios, whereas others [25, 23, 28] generally rule out the construction of wind turbines in protected landscapes.

After determining the eligible areas, a few studies further reduce it, either by a certain share [18, 19] or based on suitability factors [28, 29] per land use category of CLC [13].

Based on the identified eligible areas, the capacity can be estimated. To this end, two different methods are utilized: The majority of the analyzed studies [21, 25, 19, 26, 4, 16, 24] distribute turbines to eligible areas using a spacing distance specified by a multiple of the rotor diameter (D) in prevailing and transverse wind directions between the individual turbines. The turbine spacing ranges from 5D to 9D in the prevailing wind direction and 3D to 4D in the transverse direction. In contrast, others use fixed capacity densities, e.g., 5 MW/km² [17], 8 MW/km² [18], and 21 MW/km² [22]. Sensfuß et al. [29] and McKenna et al. [28] vary the capacity density regionally.

2.3.2. Methodology

The available area for onshore wind was determined with a greenfield land eligibility analysis (see Section 2.1). To this end, five different scenarios are defined:

Table 1
Selected exclusion criteria for the scenarios of the wind onshore potential analysis.

Criterion	Data Source	S1 ¹	S2 ²	S2a ^{2a}	S2b ^{2b}	S3 ³
Inner areas	Basis-DLM [12]	individual*	1000 m	1000 m	1000 m	1000 m
Residential buildings, outer areas	Hausumringe [35]	individual*	3 H	3 H	3 H	1000 m
Forests	Basis-DLM [12]	individual*	not excluded	not excluded	0 m	0 m
Protected Landscapes	WDPA [15]	individual*	not excluded	0 m	not excluded	0 m

¹S1 Legislation; ²S2 Expansive; ^{2a}S2a No Protected Landscapes; ^{2b}S2b No Forests; ³S3 Restrictive.
*federal state-specific exclusions

- S1 Legislation: The exclusions are defined according to the laws of Germany's federal states based on [33] and own corrections
- S2 Expansive: Wind expansion favoring exclusions including forests and protected landscapes
S2a No Protected Landscapes: S2, excluding protected landscapes
S2b No Forests: S2, excluding forests
- S3 Restrictive: Restrictive exclusions

In scenario 1, federal state-specific exclusions are applied. The exclusions for each federal state are defined in accordance with Fachagentur Wind an Land [33] with expert-based corrections and additions for keys that cannot be directly retrieved from Fachagentur Wind an Land [33]. The definition of all exclusions can be found in the supplementary data.

In scenarios 2, 2a, 2b, and 3 nation-wide exclusions are applied. Scenario S2 Expansive refers to typical buffers at the lower end of the federal state's legislation. Additionally, the construction of wind turbines in forests is allowed. Scenarios 2a and 2b build upon scenario 2, but restrict construction in protected landscapes and forests, respectively. Scenario 3 refers to exclusions on the higher end of the setback distances in the legislation. Table 1 displays the most relevant of these.

Inner areas are an influential exclusion, which refer to coherent built-up areas in accordance with §34 BauGB [34] and are modeled as the *AX_Ortslagen* features of Basis-DLM [12]. The residential buildings and other residential areas are therefore treated as areas without a development plan (outer areas). In the case of some the federal state laws, residential areas in outer areas with a statute (*Außenbereichssatzung*) are protected identical manner to inner areas. For scenario 1, we assume that all residential buildings are protected by such a statute.

Following the land eligibility analysis, areas smaller than 0.01 km² are excluded.

To estimate the capacity potential, we classify turbines with *GLAES* [36] in the eligible areas. To this end, a spacing distance of 8 D×4 D is used. A typical low wind (wind class IEC IIIB) 4.7 MW turbine with a 155 m rotor diameter and 120 m hub height is used as the reference turbine model.

Table 2
Results for the scenarios of the onshore wind potential analysis at the national level.

	S1 ¹	S2 ²	S2a ^{2a}	S2b ^{2b}	S3 ³
Area [km ²]	24663	25938	17613	10056	3923
Area Share [%]	6.89	7.25	4.92	2.81	1.10
Capacity [GW]	385	403	287	241	90
Density [$\frac{MW}{km^2}$]	15.6	15.5	16.3	23.9	22.8

¹S1 Legislation; ²S2 Expansive; ^{2a}S2a No Protected Landscapes; ^{2b}S2b No Forests; ³S3 Restrictive

2.3.3. Results & Discussion

Table 2 shows the main results of the scenarios on the national level. In scenario S2 Expansive, 7.25% of Germany's area is usable for wind turbines, which leads to a capacity potential of 404 GW. Scenario S3 Restrictive leads to only 90 GW on 1.1% of Germany's land. The capacity densities in the scenarios S1 Legislation, S2 Expansive, and S2a No Protected Landscapes are smaller than in scenarios S2b No Forests S2b and S3 Restrictive due to larger contiguous areas in the scenarios not excluding forests, i.e., S1, S2, and S2a. In the larger areas, the distance between the turbines is more apparent as smaller areas naturally promote spacing between them.

Two potential analyses on the federal state level [21, 25] are used to validate the workflow. The area potential adds up to 103.3% and 96% in relation to the study in Baden-Württemberg [25] and Northrhine-Westphalia [21], respectively. When compared with the Landesanstalt für Umwelt Baden-Württemberg [25], an Intersection over Union of 79.3% is achieved. Differences can be explained by the versions of Basis-DLM [12] and unclear definitions of single exclusions.

Figure 4 shows the range of 68 GW to 1188 GW of onshore wind potential values in literature. The results are influenced by the use of different datasets (see Section 2.2), exclusion definitions, area correction factors, and capacity estimation methods. Tröndle et al. [18], Ruiz et al. [17] and McKenna et al. [28] utilize, amongst others, CLC for land use classification, which we show to be problematic for potential analyses (Section 2.2). Furthermore, Tröndle et al. [18], in technical-social-scenarios and McKenna et al. [28] correct the estimated areas by a correction and suitability factor for land use categories, respectively. These ap-

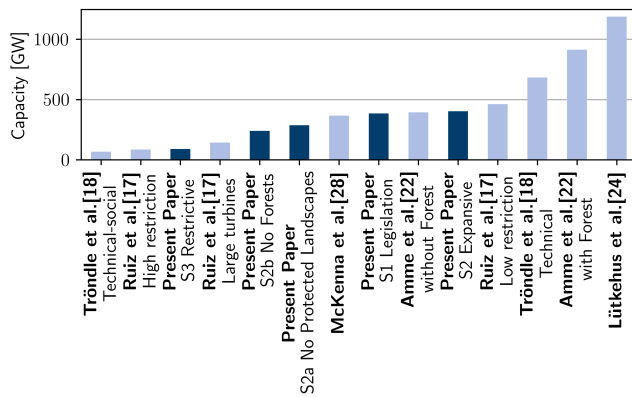


Figure 4: Comparison of onshore wind potentials for studies providing capacity potential at the national level.

proaches are not comparable to our results, which clearly indicate locations as being either eligible or ineligible. Amme et al. [22] outlined a scenario excluding residential areas with a 1000 m setback distance as well as protected landscapes but allowing forests, which is comparable to our scenario S2a No Protected Landscapes. By comparing the results, Amme et al. [22] exceed the presented eligible area and capacity by a factor of 2.47 and 3.18, respectively. Lütkehus et al. [24] use comparably low setback distances, e.g. 600 m to inner areas, and neglect residential buildings, leading to the highest capacity potential of the considered studies. This emphasizes the impact of the chosen exclusion criteria and setback distances. Furthermore, they use the land use dataset DLM250 [31] with a positional accuracy of ± 100 m.

There is no consensus on exclusions and setback distances in wind potential analyses. One exclusion used by all of the cited studies is residential areas. Nevertheless, individual residential buildings are often neglected due to data availability issues. In our scenarios, neglecting residential buildings leads to significantly higher capacity potentials (27%, 9%, 10%, 12%, and 34%). For regional or federal state analyses, this error is even more apparent: For example, in Schleswig Holstein, the potential gets overestimated by 56%, 25%, 25%, 27%, and 100%. To the knowledge of the authors, no national potential analysis with published results has considered buildings. In future work, a focus on the sensitivity regarding exclusion definitions could help make such effects more transparent. Additionally, the sensitivities of certain exclusion criteria, e.g., forests or buildings, could help legislators quantify the impact of their decisions. Our restrictive scenario results in a potential of 90 GW, which is not sufficient to reach Germany's climate goals according to different studies [3, 4, 9, 5] and underlies the importance of liberal legislation towards wind expansion.

Furthermore, the chosen turbine has a large impact on the capacity density, as well as on the land eligibility analyses via height- or diameter-dependent exclusions. We selected a typical wind turbine for low wind speeds (cf. Section 2.3.2). When using a turbine for medium wind speeds (IEC II, 5 MW capacity, 145 m diameter) with the same hub

height, the capacity potential increases by 16.2%, to 19.5%, in our scenarios. In future, site-specific turbine selection could help improve the results in this regard. Nevertheless, with respect to the chosen low wind speed turbine, the results are still robust. Only 2% and 29% of the determined locations, respectively, reach an average wind speed IEC II wind class in 100 m and 150 m height [37].

2.4. Offshore wind potential

2.4.1. Literature

The following section provides an overview of offshore wind potential analyses to be found in the literature. The regional coverage of the analyzed studies varies between global [38, 39], European [19, 18, 17, 40] and national [4]. As a first step in the potential analyses, eligible areas are determined. Most studies [39, 19, 18, 41, 40, 17] use greenfield approaches, initially considering the sea to be eligible and applying exclusion criteria. Sensfuß et al. [42], however, follow a mixed approach of greenfield analysis and pre-selected areas in their global analysis. For Germany, 80 % of the declared offshore wind areas in 4C Offshore [43] are used as pre-selected areas. Luderer et al. [4] consider the wind farm areas of the draft of the Area Development Plan 2020 [44] and areas of existing plants [45] as pre-selected ones.

The studies that follow the greenfield approach often use similar exclusion criteria, but differ in terms of dataset, methods, and buffer distances. Commonly used exclusion criteria include, amongst others, distance to shore, sea depth, protected areas, shipping routes, and infrastructures. The minimal distance to shore varies between 10 km [39] and 22.2 km [17]. The exclusion of areas with large sea depths differs between depths lower than 50 m [18, 17, 40], 100 m [17], 1000 m [39, 19, 41], or unlimited [40]. Shipping routes are excluded by Ruiz et al. [17] and Caglayan et al. [41] based on the dataset of Halpern et al. [46], which addressed the likelihood of ships. Furthermore, Caglayan et al. [41] manually exclude known routes with a buffer of 4 km. Ebner et al. [19] exclude shipping routes, but without noting a methodology or data source. Additionally, certain studies [41, 17, 39] exclude infrastructure, e.g., cables and pipelines with buffers from 500 m [41] to 7.4 km [17]. After applying the exclusion criteria, Zappa and van den Broek [40] and Tröndle et al. [18], in their technical-social, scenario reduce the resulting eligible areas to 20 % and 10 %, respectively. Zappa and van den Broek [40] explain the reduction by a set factor due to missing exclusion categories.

The potential offshore wind capacity can be estimated for the eligible areas. Most presented studies employ an aggregated method with capacity density factors ranging from 3.14 MW/km² [39] to 15 MW/km² [18]. Ebner et al. [19] reduce 14 MW/km² to 5 MW/km² due to a results deviation of a factor of 3 to the German Bundesfachplan 2017 [47, 48]. Other studies [42, 4] use a variable capacity density per eligible area. Only Caglayan et al. [41] employ a placing algorithm for wind turbines with a turbine spacing of 10 D×4 D.

2.4.2. Methodology

The offshore wind potential analysis was performed for federal states in the coastal sea and Exclusive Economic Zones (EEZ) in the Northern and Baltic sea areas. Four different scenarios were considered:

- S1 Expansive: Greenfield analyses with offshore wind expansion favoring exclusions
S1a Military: S1, including usage of military areas
- S2 Legislation: Current priority and reservation areas for offshore wind in legislation
- S3 Restrictive Legislation: Current priority areas for offshore wind in legislation

The Low Exclusion Scenarios S1 and S1a are greenfield approaches that use exclusion criteria with comparably low exclusion definitions. The following describes the main exclusions; full information about these can be found in the supplementary data. Areas within 15 km of shore and 500 m to neighboring seas are considered ineligible. To address shipping land use, the declared priority shipping areas of the current legislation of the EEZ [49] and federal states [50, 51, 52] are excluded with a buffer of 500 m. Furthermore, infrastructure facilities, e.g., cables and platforms, are excluded by CONTIS [53] with 500 m. The scenarios S1 Expansive and S1a Military differ in the consideration of designated military areas, which cover a significant share of the German coastlines. As military areas overlap with designated wind areas, a complete exclusion is unrealistic. However, the exclusion of individual sub-areas is not possible due to a lack of indications of the suitability of mixed use. Only Scenario S1 Expansive further excludes declared military areas according to CONTIS [54] and ROP [49].

The scenario S2 Legislation considers all designated areas for offshore wind as pre-selected, whereas scenario S3 Restrictive Legislation only considers the priority and conditional priority areas ones. The definition of these areas is based on the current legislation of the EEZ [49], Lower Saxony [50], and Mecklenburg-Western Pomerania [51]. Schleswig Holstein and Hamburg do not designate areas for offshore wind [55, 56]. The Legislation scenarios S2 and S3 further apply the infrastructure exclusions described in Low Exclusion Scenarios S1 and S1a.

After employing the exclusions of the scenarios, areas smaller than 0.1 km² are excluded.

The potential capacity of the scenarios is estimated with a similar approach as that used for onshore wind (Section 2.3.2) by using the turbine placement of *GLAES* [36] and a turbine spacing of 8D×4D, respectively. A reference turbine with a capacity of 8 MW and a rotor diameter of 167 m is used.

2.4.3. Results & Discussion

The results of the offshore potential analysis on the national level are presented in Table 3 and show a range of between 34.1 GW (S3 Restrictive Legislation) and 99.6 GW (S1a Military).

Table 3

Results for the scenarios of the offshore wind potential analysis on a national level

	S1 ¹	S1a ^{1a}	S2 ²	S3 ³
Area [km ²]	7353	9275	5174	3182
Area Share [%]	13.07	16.48	9.19	5.65
Capacity [GW]	79.1	99.6	55.8	34.1
Density [$\frac{MW}{km^2}$]	10.75	10.74	10.79	10.71

¹S1 Expansive; ^{1a}S1a Military; ²S2 Legislation; and ³S3 Restrictive Legislation

It can be noted that there exists the possibility to increase the potential from current legislation, i.e. S2 and S3, by limiting other declared land uses such as shipping or military areas. However, the possible increase in capacity potential highly differs between the Northern and Baltic seas. From scenario S2 Legislation to S1 Expansive the potential is increased by 21.6 GW in the North Sea and 1.6 GW in Baltic. For the comparison of S2 Legislation to S1a Military, the capacity increase is higher, with 39 GW and 5 GW, respectively. Thus, by redefining and limiting other declared land uses in legislation as military or shipping areas, further areas could be designated for offshore wind, especially in the North Sea. Future work could critically revise these areas or consider combined usage with offshore wind projects.

Furthermore, the reference turbine impacts the capacity potential. In the future, site-specific turbine designs and a sensitivity analysis for turbine selection could be applied.

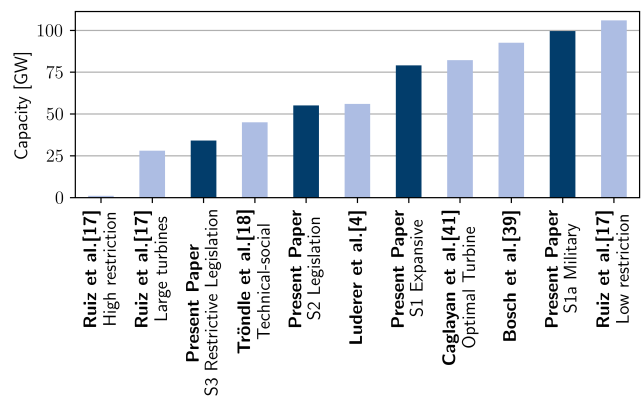


Figure 5: Comparison of offshore wind potentials for studies providing capacity potential on the national level

The results of the presented scenarios are compared to the literature in Figure 5. The scenarios S1 Expansive and S1a Military follow a greenfield approach, comparable to all considered studies except for that of Luderer et al. [4]. Luderer et al. [4], who use the same designated wind farm area of BSH leading to 56 GW, comparable to 55.8 GW in the present scenario, S2 Legislation.

For the greenfield analyses, none of the presented studies use official German data, e.g., for shipping or military areas. Two scenarios of Ruiz et al. [17] and the technical-

social scenario of Tröndle et al. [18] even undercut the capacity potential results of our scenarios S2 Legislation and S3 Restrictive Legislation. Ruiz et al. [17] in their low exclusion scenario and Bosch et al. [39] have comparable capacity potentials to S1a. However, as the capacity densities of our study are around two and three times higher in comparison to their studies, respectively, this indicates significantly fewer eligible areas in our scenarios. The comparisons show the impact of data sources, exclusions, and capacity densities on the land eligibility analyses and capacity estimations.

2.5. Open-field photovoltaic potential

2.5.1. Literature

Although wind potential analyses mostly use greenfield approaches in land eligibility analysis (see Section 2.3), open-field PV potential analyses often first consider pre-selected areas as being eligible and then apply further exclusion criteria [57, 17, 18, 19, 58, 59, 22, 4]. Only a few potential analyses choose a greenfield exclusion approach [20, 60].

However, as the pre-selected areas highly differ across the studies, several examples are presented: Ruiz et al. [17] and Tröndle et al. [18] estimate the potential for Europe and consider land use categories as pre-selected areas, which leads to a high area potential for open-field PV. Ruiz et al. [17] define amongst others, bare land, some cropland, and some eligible classes of vegetation and use a combination of Global Land Cover [61] and Corine Land Cover [13] to identify these. This leads to an initial eligible area of 44% of Germany, from which a share of 3% is considered eligible in another scenario. Tröndle et al. [18] consider 10% of bare and unused land defined by GlobeCover2009 [62] as pre-selected areas in a technical-social potential analysis. Lux et al. [57] define certain shares of categories of CLC [13] eligible, e.g., 16% of bare land and 2% of bushland. Meanwhile, Ebner et al. [19] consider agriculture and grazing land identified by CLC [13] in less favored regions [63] eligible for technical potential. However, this is further reduced to 7% of the pre-selected area, which is 50% of the area share currently used for energy crops. Several studies with the scope of Germany follow the legislation of the Renewable Energy Act (EEG) [64]. Amongst other areas, the EEG considers less-favored areas and side strips of motorways and railways to be eligible. The potential areas along side strips are either defined by a 110 m width in accordance with EEG 2017 [65] or a 200 m width in accordance with EEG 2021 [64] minus a 15 m animal migration buffer. Luderer et al. [4] also use side strips, but consider 185 m around the line objects of OSM, therefore neglecting the width of the road and the animal migration corridor. Furthermore, they consider agricultural land with poor soil quality, which is defined with the dataset Soil Quality Rating (SQR) [66] and a threshold of 40. Amme et al. [22] similarly consider the less-favored areas, but also consider side strips with a width of 500 m, which corresponds to 2.7 times the current legislation. Agricultural land with higher soil quality rating than 40 are excluded within the side strips. Other EEG-favored areas are also neglected due to data availability and small

resulting areas. Several studies perform potential analyses on a federal state level in Germany, e.g., Seidenstücker [59] for North Rhine-Westphalia and Landesanstalt für Umwelt Baden-Württemberg [58] for Baden-Württemberg. Both studies use input datasets with local coverage and high resolutions, e.g., Basis-DLM [12], and estimate the potential for the side strips of 110 m of rails and road ways in accordance with the legislation of EEG 2017 [65].

After defining the pre-selected areas, further exclusion criteria can be applied, resulting in eligible areas of various shapes and sizes. As it is not economically-feasible to install open-field PV sites in small eligible areas, several studies exclude areas smaller than a certain threshold. The threshold can vary in the range from 500 m² [59] to 100.000 m² [22].

As the second step of the potential analysis, the installable open-field PV capacity on eligible areas is estimated. Open-field PV potential analysis uses an empirical factor of the capacity density in MW/km². However, the literature reports a high range from 40 MW/km² in [19] to 300 MW/km² [17]. Ebner et al. [19] explain the factor of 40 MW/km² based on aerial photo evaluation of existing open-field PV systems. Tröndle et al. [18] explain their value of 80 MW/km² with a module efficiency of 16% and 50% area reduction by row placements to prevent shadowing. Seidenstücker [59] assume a module efficiency of 17% and also an area reduction of 50% for slopes less than 20°, leading to 85 MW/km². Wirth [67] reports a value of 100 MW/km² based on row spacing and a module efficiency of 20%.

2.5.2. Methodology

In the first step of the potential analysis for open-field PV pre-selected areas are considered eligible followed by further exclusions. To this end three scenarios are regarded:

- S1 Side Strips: Side strips of motorways and railways in accordance with the subsidy areas of the EEG 2021 [64]
- S2 Poor Soil: Arable land with barren soil based on the Soil Quality Rating (SQR) of [66]
- S3 Combination: Side strips, for which arable land is restricted to SQR < 40, and S2

Scenario S1 Side Strips estimates the potential of the side strips of motorways and railways. Their routes and widths are identified by Basis-DLM [12]. Then, side strips of 200 m are used, from which 15 m on the inside is subtracted for animal migration. The remaining area represents the pre-selected area.

Scenario S2 Poor Soil pre-selects arable land with a bad soil quality based on the SQR dataset [66]. The SQR threshold was chosen to be 30 based on a pre-analysis. Figure 6 shows the area potential and share of arable land for SQR limits of between 20 and 50. As is shown in Section 2.5.1, other potential studies use a threshold of 40, which results in 6.28% of arable land. We assume this to be too ambitious due to land use conflicts with cultivation of arable land and therefore choose the threshold of 30. All areas up to

Table 4
Selected exclusion criteria for the scenarios of the open-field PV potential analysis.

Criterion	Data Source	S1 Side Strips	S2 Poor Soil	S3 Combination
Forests	Basis-DLM [12]	10 m	10 m	10 m
All Buildings	Hausumringe [35]	10 m	10 m	10 m
Arable land	Basis-DLM [12], SQR [66]	not excluded	$SQR \geq 30$	$SQR \geq 30$, Sidestripes: $SQR \geq 40$
Motorways, Railways	Basis-DLM [12]	15 m	200 m	15 m

a selected SQR value are intersected with the arable land in Germany from Basis-DLM [12] due to the resolution of 100 m×100 m in the BGR rating [66].

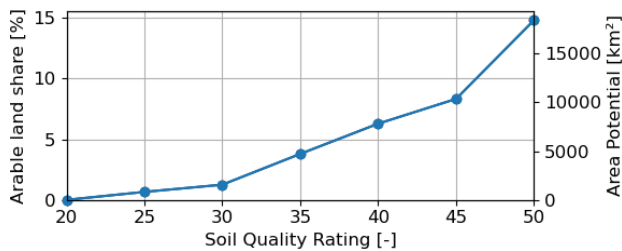


Figure 6: Sensitivity analysis of the Soil Quality Rating threshold for arable land in the land eligibility analysis for open-field PV.

Scenario S3 Combination is a combination of a pre-selection using side strips and arable land with barren soil. As side strips are considered less valuable than other areas, arable land with SQR values of less than 40 are excluded. On all other arable land, only SQR values of less than 30 are used as a pre-selection. It should be noted that other land uses than agricultural inside the side strips are not restricted by the SQR rating.

After identifying pre-selected eligible areas for each scenario, unsuitable areas within these are deducted by further exclusion criteria. Table 4 displays the most relevant exclusions. The definition of all exclusions can be found in the supplementary material. After the land eligibility analysis, eligible areas smaller than a threshold of 5000 m² were excluded for economic reasons, which lies within the range of the presented literature (see Section 2.5.1). However, this area threshold leads to a deviation of eligible areas at the different regional levels. Areas may become ineligible if split by a border to a size lower than the threshold, whereas on a higher regional level still eligible. For the three scenarios, this leads to a capacity deviation from 1.3% to 1.5% between the federal state and the municipality level.

As a next step in the potential analysis, the installable capacity on the eligible land was estimated. Therefore, the eligible areas and their size A_{OFPV} are extracted, on which the modules are placed in a southerly direction with an optimal tilt for the latitude, which is calculated using the *RESKit* tool [11] in accordance with Ryberg [60]. This area can be converted by taking a factor for row spacing $f_{RS} = 0.5$, a factor for construction-related obstructions, e.g., access roads or surrounding areas, $f_c = 0.72$ [68], and the efficiency of

Table 5
Results for the scenarios of the open-field PV potential analysis at the national level.

	S1 ¹	S2 ²	S3 ³
Area [km ²]	5723	1560	4373
Area Share [%]	1.60	0.44	1.22
Capacity [GW _p]	456.1	123.6	347.7
No. of Municipalities	11003	11003	11003
...with pre-selected areas	5667	1892	6446
...with potential	5253	1711	5939

¹S1 Side Strips; ²S2 Poor Soil; and ³S3 Combination.

the modules, which is assumed to be $\eta_{PV} = 0.22$ in line with current high-end modules [69, 70], into consideration:

$$\begin{aligned}
 P_{OFPV} &= \eta_{OFPV} \cdot f_{RS} \cdot f_c \cdot A_{OFPV} \\
 &= 79.2 \text{ MW/km}^2 \cdot A_{OFPV}
 \end{aligned} \quad (3)$$

2.5.3. Results & Discussion

The results at the national level for the potential area and the capacity of the scenarios are shown in Table 5. The capacity potential varies between 123.6 GW_p in S2 Poor Soil and 456.1 GW_p in S1 Side Strips.

To validate the presented workflow, two potential analyses for the federal state level [58, 59] were used due to their high spatial resolutions and usage of local data. Similarly to Side Strips S1, the studies consider pre-selected areas at the sides of roads and railways. Using similar exclusion criteria and datasets as the corresponding studies, an Intersection over Union of 81.38% for Landesanstalt für Umwelt Baden-Württemberg [58] and 87.88% for Seidenstücker [59] were achieved. The area potential of the presented workflow in relation to that reported by [58] and [59] is 88% and 103%, respectively. Remaining differences between the results of the studies and this paper arise due to different versions of land cover datasets and unclear definitions of single exclusions.

As is shown in Figure 7, the literature provides a high range of 90 GW_p [18] to 1285 GW_p [17] as capacity potentials for open-field PV, because the pre-selected areas, used datasets, area reduction factors, and applied exclusion criteria highly differ between the studies (cf. Section 2.5.1). Furthermore, the used capacity density factors vary greatly between the studies, which leads to further deviations. Ruiz et al. [17] and Tröndle et al. [18] use set shares, 3% and 10%,

respectively, of large land use categories for the land eligibility analyses, and are therefore not comparable to our scenarios.

Methodology-wise our presented scenarios are only comparable to Amme et al. [22]. For the presented SQR scenario, the higher potential capacity of Amme et al. [22] can be explained by its higher SQR threshold. For the side strips scenario, Amme et al. [22] use side strips that are 2.7 times the width of current legislation. Nevertheless, by additionally excluding areas with a SQR higher than 40, the resulting capacity is lower than in our scenario S1 Side Strips.

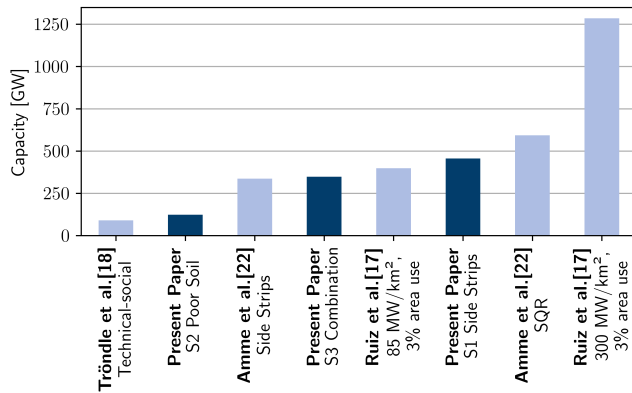


Figure 7: Comparison of open-field PV potentials for studies providing capacity potential at the national level.

The presented workflow could be further extended by considering other subsidy-areas of the Renewable Energy Act [64] like dumps and landfills as pre-selected areas. Furthermore, categories beyond the scope of current legislation could be chosen as pre-selected areas. However, there exists no consensus in the literature about eligible land use categories and considering entire categories eligible tend to lead to high potentials, as in Ruiz et al. [17]. Such high area shares are critical due to the land use conflicts they can induce: Whereas wind turbines only occupy a share of their designated areas, open-field PV plants cover most of their appointed ones, which can lead to conflicts with, for example, agricultural land use. Furthermore, legislation has a significant impact on the distribution of potentials. Especially in the open-field PV scenarios, many municipalities have no potential (cf. Table 5), due to the limitation to municipalities with subsidy-eligible areas. This can lead to unequally-distributed economic benefits among municipalities, as well as higher resistance in society because of visual impacts, for instance. As the results are also highly sensitive towards the chosen capacity density factor, one avenue of further work could be to incorporate future system designs. Additionally, the effect of placing the modules flat or in an east-west orientation without any row-spacing could be analyzed.

3. Rooftop photovoltaic potential

In the following chapter, the assessment of rooftop PV potential for Germany is discussed. First, an overview of

the literature is given (Section 3.1). Then, the methodology to extract potential from 3D building data is described (Section 3.2). The results are then presented and discussed (Section 3.3).

3.1. Literature

Rooftop PV potential analyses can be classified by their geographical extent and the resolution of their results [71, 72].

The resolution of different approaches can be split into high, medium, and low levels. High level approaches, which can assess the potential for individual buildings include, for example, image recognition techniques [73, 74, 75, 76] or workflows using 3D building models [77, 78, 79, 80, 81]. For instance, Grothues and Seidenstücker [77] determine all roof geometries in North Rhine-Westphalia on the basis of laser scan data at 0.5 m×0.5 m resolutions. Low- and medium-level approaches base their analysis mostly on statistical data and are therefore limited to the assessment of potentials for the regional scope of the data, e.g., to regions, countries, or raster resolution [17, 18, 20, 72, 82, 83, 84, 19, 85]. Tröndle et al. [18], for instance, use population data from the European Settlement Map [27] to estimate roof areas and calibrate them with data from sonnendach.ch [86]. Meanwhile, Ruiz et al. [17] use CLC [13] data to identify residential and industrial areas in which they estimate roof areas based on fixed factors.

The geographical extent of these analyses varies from single buildings to continent-wide. Statistical approaches are mainly used to perform large-scale analyses, such as at national [20, 72, 19, 85] or continental scales [17, 18, 84]. However, more recent studies were able to apply high-level methodologies to the national scale. Walch et al. [79] use LoD2 3D data to extract rooftop PV potential in Switzerland. To this end, they calculate the area and orientations of 9.6 million rooftops directly from the data. Luderer et al. [4] estimate the rooftop PV potential in Germany at the municipality level by correlating it with building footprints in a region. Similarly, Wiehe et al. [26] used building footprints in Germany and building use to estimate generation potential. Eggers et al. [87] use LoD1 building models (without information on rooftop geometry) to estimate German rooftop PV potential.

Approaches, that use data without information about superstructures, e.g., chimneys and windows, on roofs to estimate the available roof area, utilize reduction factors to adapt the potentially usable areas. Mainzer et al. [72] use a factor of 0.58 to exclude obstacles on roofs and in areas with too much shadowing. In turn, Fath et al. [80] differentiates between flat (0.7) and tilted (0.75) roofs based on the work of Kaltschmitt [88]. The International Energy Agency (IEA) [89] determines a factor of 0.6 for constructions, shading, and historical elements. Walch et al. [79] estimate the factor from LoD4 data in Geneva (38,000 roofs) with a machine learning approach for other LoD2 building models and estimate the factor to be between 0 and 0.8 depending on the roof size and tilt. Portmann et al. [86] distinguish between

flat (0.7) and tilted (0.42 – 0.8) roofs, for which a differentiation between roof size and category is carried out. Eggers et al. [87] use a factor of 0.486 to account for obstructions, shading, and inefficiencies when placing the modules. Wiehe et al. [26] assume that 60% of the roof area on residential and 80% of the roof area on industrial and commercial structures are usable. Grothues and Seidenstücker [77] estimate the impact of obstructions directly based on a highly resolved (0.5 m × 0.5 m) digital elevation model.

In contrast to land eligibility analyses (see Section 2), in which a clear workflow has been established, the methodologies between different rooftop PV potential analyses vary greatly. Many high-resolution approaches have been used to estimate potential on a smaller geographical scale. To the best of the authors' knowledge, no rooftop PV potential analysis has been performed using 3D building models with roof geometries for all of Germany.

3.2. Methodology

In the present study we used 3D building models based on LiDar in the CityGML format with level of detail (LoD) 2 [90] of the Bundesamt für Kartographie und Geodäsie (BKG) [91] (high resolution) to estimate rooftop PV potential in Germany (high geographical extent). To this end, 93.1 million roofs were evaluated to estimate Germany's rooftop PV potential. LoD2 corresponds to simplified building geometries with standardized roof shapes [92]. Therefore, the orientation of the roof, i.e., the tilt and azimuth, can be estimated. However, information regarding superstructures reducing the usable area for rooftop PV is missing.

In order to extract tilt and azimuth from roof geometries, the normal vector on the plane of the geometry is determined. The north-based azimuth is defined as the angle between the north vector and x-y part of the normal vector:

$$azi = \arccos(\vec{n} \cdot [0, 1, 0]^T) \quad (4)$$

The tilt can be determined by calculating the angle between the z-vector and normal vector:

$$tilt = \arccos(\vec{n} \cdot [0, 0, 1]^T) \quad (5)$$

To further estimate the potential to install PV modules on rooftops, in a first step the area of the roof geometries was directly retrieved from the data. However, the usable area for rooftop PV is limited by shading or obstacles like windows or chimneys, which is taken into account by incorporating a factor. In this paper, the factor was set to $fac_{area} = 0.6$, which is in accordance with literature values. The capacity potential of individual roofs is estimated by placing modules with an efficiency of $\eta = 0.22$ (see Section 2.5.2). Moreover, roofs with tilts lower than 10° are assumed to be flat. Modules on flat roofs are placed in a southerly direction with an optimal tilt angle in accordance with Ryberg [60]. For row spacing on flat roofs, an additional factor of $fac_{RS} = 0.5$ is employed. The capacity calculation for single roofs can be summarized as follows:

$$P_{PV,peak} = \begin{cases} 0.6 \cdot \eta_{PV} \cdot A_{roof}, & \text{for tilt} \geq 10^\circ \quad (6a) \\ 0.6 \cdot 0.5 \cdot \eta_{PV} \cdot A_{roof}, & \text{for tilt} < 10^\circ \quad (6b) \end{cases}$$

Areas, that correspond to less than 1 kW_p capacity are excluded from the potential. This translates to an area threshold of 7.6 m^2 for tilted roofs and 15.2 m^2 for flat ones. The potentials in **trep-db** are published in groups for each municipality, nuts3-region, and federal state, but not individually for each building due to the large overhead storage. To this end, a fixed grouping method is used: One flat group includes all items up to a tilt angle of 20° . Eight azimuth groups (North (N), North-West (NW), West (W), South-West (SW), South (S), South-East (SE), East (E), and North-East (NE)) contain all elements from $20\text{-}90^\circ$ in the respective directions. For rooftop PV, no scenarios are considered, but the **trep-db** includes two datasets, representing two scenarios:

- All roofs
- No northern roofs: Exclusion of north facing groups (N,NW,NE)

3.3. Results & Discussion

Based on the presented workflow, a potential of 625 GW_p is estimated for all rooftops in Germany. However, the potential decreases to 492 GW_p if north-facing groups are excluded.

Figure 8 and Figure 9 demonstrate the capacity-weighted potential distribution of the azimuth angle and tilt angle for saddle roofs. The cardinal directions show the highest capacity potential. A substantial capacity potential is located on northern facing roofs. Figure 9 shows the distribution

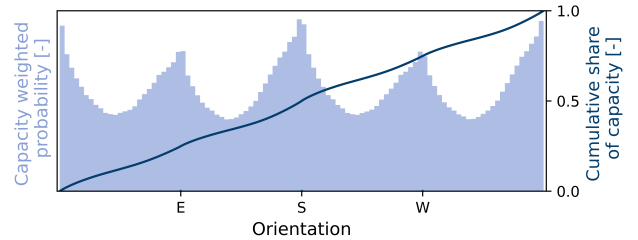


Figure 8: Capacity weighted azimuth distribution of German roofs.

of the capacity weighted potential distribution of the tilt angle. As only saddle roofs are considered for the plots, only tilt angles from 10° upwards are present. The main capacity potentials can be observed up to a tilt angle of 45° (see Figure 9).

To validate the presented workflow, the results for the federal state North Rhine-Westphalia are compared against Grothues and Seidenstücker [77]. When aligning the workflows by lowering the efficiency to 17%, using $f_{RS} = 0.4$ and applying the same limit for areas (7 m^2 for tilted roofs and 17.5 m^2 for flat ones) the capacity of roofs in North Rhine-Westphalia adds up to 84.0 GW_p , which is comparable to the 81.4 GW_p estimated by Grothues and Seidenstücker [77]. It should be noted that Grothues and Seidenstücker [77] exclude rooftops with an irradiation lower than 814 kWh/m^2 ,

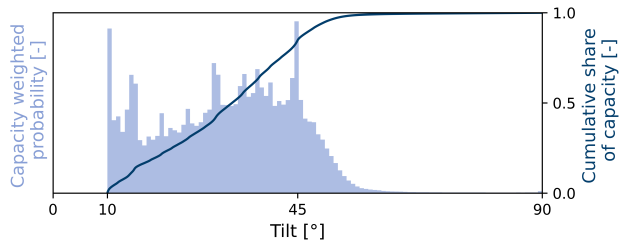


Figure 9: Capacity-weighted tilt distribution of German roofs.

which is not reproduced, and therefore a higher result is to be expected. Furthermore, the potential reduction due to roof obstructions is not comparable in the two studies.

Figure 10 presents the Germany-wide capacity potential of rooftop PV in this paper and other studies. The comparison shows a range of 43 GW_p [17] to 746 GW_p [18]. However, comparability between the studies is limited. The studies significantly differ in their methodologies for rooftop area estimations and assumptions as the reduction factor for superstructures and efficiency in the capacity estimation. Furthermore, some studies only consider the rooftop PV potential for individual building categories, e.g., residential in Mainzer et al. [73]. The only capacity potential, which has been estimated by a high resolution approach (see Section 3.1) assumes 504 GW [87], which is of similar magnitude to the potentials estimated in our approach.

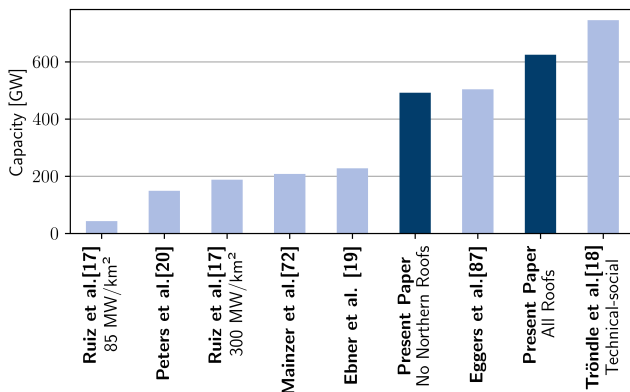


Figure 10: Comparison of rooftop PV potentials for studies providing capacity potential at the national level.

In future, the estimation of unusable areas on roofs can be improved when LoD3/LoD4-data becomes available for Germany. Alternatively, as proposed by Walch et al. [79], the LoD4-Dataset from Geneva could be used to estimate the share of unusable roof areas by means of a machine learning approach.

4. Discussion

The capacity estimations of the reviewed literature for different technologies in Germany are shown in Figure 11. The potentials exhibit large variations between the studies

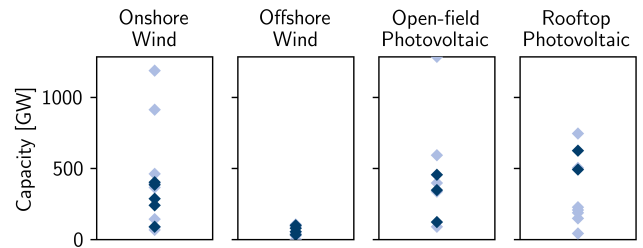


Figure 11: Potential capacities of different potential studies on the national level for onshore wind, offshore wind, open-field photovoltaic, and rooftop photovoltaic.

and scenarios. Our data analysis (Section 2.2) shows one reason for the present deviations: the used input datasets make the findings of different studies using different datasets hardly comparable. Another reason for the significantly deviating potentials is the chosen exclusion criteria and the corresponding buffers. Neglecting residential buildings in wind potential analyses, for example, can lead to considerable over-estimations. In future work, a sensitivity analysis regarding the criteria could help quantify the effects in a more in-depth manner. Nevertheless, without applying high-quality datasets, the conclusions would not be meaningful. In other regions of the world, OSM may not be as comprehensive and a dataset with official characteristic such as Basis-DLM may not be available. In future work, worldwide high-resolution datasets should be used to reevaluate global renewable potentials.

Figure 12 shows the spatial distribution of the capacity potential in Germany's municipalities for one scenario of onshore wind, open-field PV, and rooftop PV, which visualizes the spatial heterogeneity of the results. Additionally, Figure 13 shows the cumulative share of Germany's municipalities over all scenarios for the regarded technologies and the impact of boundary conditions, e.g., pre-selected areas or exclusions, on regional potentials in municipalities. For the wind scenarios, the share of municipalities without potential highly differs between 28% and 70%, showing the high impact of the exclusion criteria on the regional level. For all open-field PV scenarios, a large number of municipalities are without potentials, whereas rooftop PV potentials are more equally distributed. As is shown on the right-hand side of the figure, the maximum capacities found in the municipalities highly vary for the technologies and scenarios between 634 MW (On. Wind, S3 Restrictive) and 9.3 GW (Rooftop PV, All Roofs). For the use case of energy system models, the unequal distribution of potentials in municipalities emphasizes the importance of detailed and qualitative potentials for regional analyses.

5. Conclusions

The first time evaluation of land use datasets and the proposed renewable potential scenarios reveal significant biases in the datasets that are commonly applied by the energy sys-

Impact of Data Quality on Renewable Energy Potential Estimations

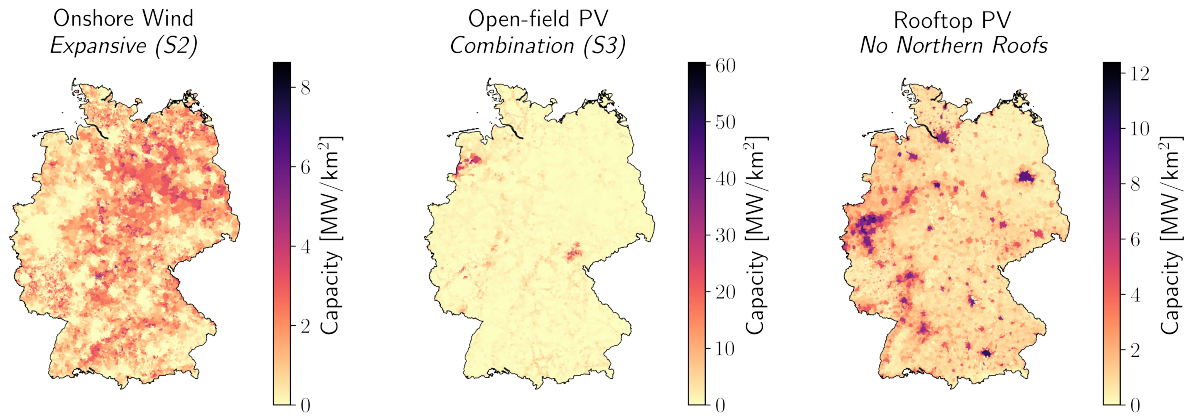


Figure 12: Potential capacity density in Germany's Municipalities for different technologies.

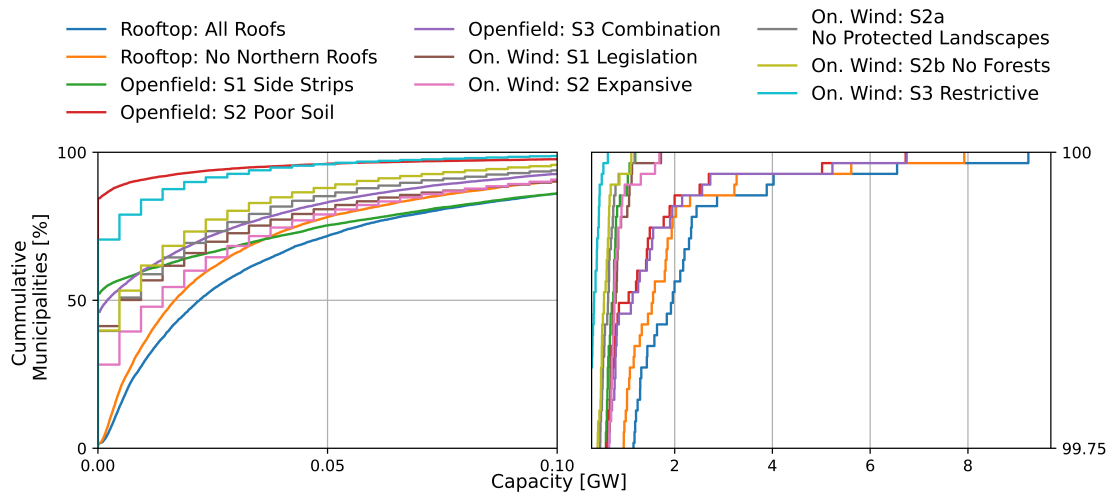


Figure 13: Cumulative municipalities over capacity potential for the scenarios of open-field, rooftop PV and wind onshore.

tems community: The use of Corine Land Cover [13] leads to a significant overestimation of the potentially usable area for renewable energy technologies by a factor of 4.6 to 5.2 in comparison to Basis-DLM [12] and Open Street Map [14], respectively. High-quality datasets are needed to supply reliable input for policy-makers or energy system models. In the case of Germany, Basis-DLM [12] and Open Street Map [14] provide similar information for several categories, especially line-like features, such as power lines or railways. For others, Basis-DLM and Open Street Map show significant differences, e.g., industry/commercial, lakes, or rivers. Furthermore, the impact of several exclusion criteria is apparent in the presented scenarios and variations. For example, the disregard of residential buildings in onshore wind analyses leads to an overestimation of the capacity by up to 34% for our scenarios.

The presented scenarios for onshore wind, offshore wind, open-field, and rooftop photovoltaic are published in the open access database **trep-db**. For rooftop photovoltaic, the potentials are estimated by CityGML Level of Detail 2 data for

the first time, which leads to a 492 GW_p potential capacity when northerly-facing roofs are excluded.

This work should motivate improvement in the internationally-available land use datasets, as their quality has a significant impact on the correct design of regulations for renewable resource emplacements.

6. Acknowledgements

This work was supported by the BMWi (German Federal Ministry of Economic Affairs and Energy) [promotional reference 3EE5031D]; and the Helmholtz Association under the program “Energy System Design.”

References

- [1] United Nations, Paris Agreement, Technical Report, United Nations, Paris, 2015. URL: https://unfccc.int/sites/default/files/english_paris_agreement.pdf.
- [2] Bundes-Klimaschutzgesetz (KSG), 2021. URL: <https://www.gesetze-im-internet.de/ksg/ksg.pdf>.
- [3] D. Stolten, P. Markewitz, T. Schöb, L. Kotzur, Strategien für eine treibhausgasneutrale Energieversorgung bis zum Jahr 2045. (Kurzfassung), Technical Report, Forschungszentrum Jülich GmbH, Jülich, 2021. URL: https://www.fz-juelich.de/iek/iek-3/DE/_Documents/Downloads/transformationStrategies2045ShortStudy.pdf?__blob=publicationFile.
- [4] G. Luderer, C. Kost, D. Sörgel, Deutschland auf dem Weg zur Klimaneutralität 2045 - Szenarien und Pfade im Modellvergleich, Technical Report, 2021. URL: https://publications.pik-potsdam.de/pubman/item/item_26056, artwork Size: 359 pages Publisher: Potsdam Institute for Climate Impact Research.
- [5] J. Brandes, M. Haun, D. Wrede, P. Jürgens, C. Kost, H.-M. Henning, H.-M. Henning, H.-M. Henning, Wege zu einem klimaneutralen Energiesystem - Die deutsche Energiewende im Kontext gesellschaftlicher Verhaltensweisen - Update November 2021: Klimaneutralität 2045, Technical Report, Fraunhofer-Institut für Solare Energiesysteme IS, Freiburg, 2021.
- [6] M. Kendziorowski, L. Göke, C. Kemfert, von Hirschhausen, E. Zozmann, 100% erneuerbare Energie für Deutschland unter besonderer Berücksichtigung von Dezentralität und räumlicher Verbrauchsnähe – Potenziale, Szenarien und Auswirkungen auf Netzinfrastrukturen, Technical Report, Deutsches Institut für Wirtschaftsforschung, Berlin, 2021.
- [7] Prognos, Öko-Institut, Wuppertal-Institut, Klimaneutrales Deutschland 2045 Wie Deutschland seine Klimaziele schon vor 2050 erreichen kann, Technical Report, Agora Energiewende und Agora Verkehrswende, 2021. URL: https://static.agora-energiewende.de/fileadmin/Projekte/2021/2021_04_KNDE45/A-EW_209_KNDE2045_Zusammenfassung_DE_WEB.pdf.
- [8] M. Fette, C. Brandstät, H. C. Gils, H. Gardian, T. Pregger, J. Schaffert, E. Tali, N. Brücken, Multi-Sektor-Kopplung - Modellbasierte Analyse der Integration erneuerbarer Stromerzeugung durch die Kopplung der Stromversorgung mit dem Wärme-, Gas- und Verkehrssektor, Technical Report, Fraunhofer-Institut für Fertigungstechnik und Angewandte Materialforschung IFAM, Deutsches Zentrum für Luft- und Raumfahrt e.V. (DLR), Gas- und Wärme-Institut Essen e.V., 2020. URL: <https://elib.dlr.de/135971/1/MuSeKo-Endbericht-2020-08-31.pdf>.
- [9] L. Göke, C. Kemfert, M. Kendziorowski, C. V. Hirschhausen, 100 Prozent erneuerbare Energien für Deutschland: Koordinierte Ausbauplanung notwendig, Technical Report, 2021. URL: http://www.diw.de/sixcms/detail.php?id=diw_01.c.821878.de, publisher: DIW - Deutsches Institut für Wirtschaftsforschung Version Number: 2.0.
- [10] R. McKenna, S. Pfenninger, H. Heinrichs, J. Schmidt, I. Staffell, C. Bauer, K. Gruber, A. N. Hahmann, M. Jansen, M. Klingler, N. Landwehr, X. G. Larsén, J. Lilliestam, B. Pickering, M. Robinius, T. Tröndle, O. Turkovska, S. Wehrle, J. M. Weinand, J. Wohland, High-resolution large-scale onshore wind energy assessments: A review of potential definitions, methodologies and future research needs, *Renewable Energy* (2021) S0960148121014841. URL: <https://linkinghub.elsevier.com/retrieve/pii/S0960148121014841>. doi:10.1016/j.renene.2021.10.027.
- [11] D. Ryberg, M. Robinius, D. Stolten, Evaluating Land Eligibility Constraints of Renewable Energy Sources in Europe, *Energies* 11 (2018) 1246. URL: <http://www.mdpi.com/1996-1073/11/5/1246>. doi:10.3390/en11051246.
- [12] [dataset] Geobasisdaten: © GeoBasis-DE / BKG (2021), Digitales Basis-Landschaftsmodell (Ebenen) (Basis-DLM) (2021).
- [13] [dataset] Copernicus Programme, CORINE Land Cover (CLC) (2018). URL: <https://land.copernicus.eu/pan-european/corine-land-cover>.
- [14] [dataset] OpenStreetMap contributors, Open Street Map (2021). URL: <https://www.openstreetmap.org/>.
- [15] [dataset] UNEP-WCMC, IUCN, The world database on protected areas (2016). URL: <https://www.protectedplanet.net/23>.
- [16] F. Masurowski, M. Drechsler, K. Frank, A spatially explicit assessment of the wind energy potential in response to an increased distance between wind turbines and settlements in Germany, *Energy Policy* 97 (2016) 343–350. URL: <https://linkinghub.elsevier.com/retrieve/pii/S0301421516303718>. doi:10.1016/j.enpol.2016.07.021.
- [17] P. Ruiz, W. Nijs, D. Tarvydas, A. Sgobbi, A. Zucker, R. Pilli, R. Jonsson, A. Camia, C. Thiel, C. Hoyer-Klick, F. Dalla Longa, T. Kober, J. Badger, P. Volker, B. Elbersen, A. Brosowski, D. Thrän, ENSPRESO - an open, EU-28 wide, transparent and coherent database of wind, solar and biomass energy potentials, *Energy Strategy Reviews* 26 (2019) 100379. URL: <https://linkinghub.elsevier.com/retrieve/pii/S2211467X19300720>. doi:10.1016/j.esr.2019.100379.
- [18] T. Tröndle, S. Pfenninger, J. Lilliestam, Home-made or imported: On the possibility for renewable electricity autarky on all scales in Europe, *Energy Strategy Reviews* 26 (2019) 100388. URL: <https://linkinghub.elsevier.com/retrieve/pii/S2211467X19300811>. doi:10.1016/j.esr.2019.100388.
- [19] M. Ebner, C. Fiedler, F. Jetter, T. Schmid, Regionalized Potential Assessment of Variable Renewable Energy Sources in Europe, in: 2019 16th International Conference on the European Energy Market (EEM), IEEE, Ljubljana, Slovenia, 2019, pp. 1–5. URL: <https://ieeexplore.ieee.org/document/8916317/>. doi:10.1109/EEM.2019.8916317.
- [20] D. W. Peters, S. Schicketanz, D. M. Hanusch, A. Rohr, M. Kothe, P. Kinast, Räumlich differenzierte Flächenpotentiale für erneuerbare Energien in Deutschland, Technical Report, Bundesministerium für Verkehr und digitale Infrastruktur (BM, Berlin, 2015. URL: https://www.bbsr.bund.de/BBSR/DE/veroeffentlichungen/ministerien/bmvi/bmvionline/2015/BMVI_Online_08_15.html.
- [21] Landesamt für Natur, Umwelt und Verbraucherschutz Nordrhein-Westfalen (LANUV), Potenzialstudie Erneuerbare Energien NRW – Windenergie, 2021. URL: https://www.lanuv.nrw.de/fileadmin/lanuvpubl/1_infoblaetter/Handout_Potenzialstudie_Windenergie_Druck.pdf.
- [22] J. Amme, E. Kötter, F. Janiak, B. Lancien, Der Photovoltaik- und Windflächenrechner - Methoden und Daten (2021). URL: <https://zenodo.org/record/4731921>. doi:10.5281/ZENODO.4731921, publisher: Zenodo Version Number: v1.0.
- [23] D. S. Ryberg, Z. Tulemat, D. Stolten, M. Robinius, Uniformly constrained land eligibility for onshore European wind power, *Renewable Energy* 146 (2020) 921–931. URL: <https://linkinghub.elsevier.com/retrieve/pii/S0960148119309619>. doi:10.1016/j.renene.2019.06.127.
- [24] I. Lütkehus, H. Salecker, K. Adlunger, Potenzial der Windenergie an Land, Technical Report, Umweltbundesamt, Dessau-Roßlau, 2013.
- [25] Landesanstalt für Umwelt Baden-Württemberg, Potenzialanalyse der Windenergie an Land, 2019. URL: <https://www.energieatlas-bw.de/wind/potenzialanalyse/uberblick>.
- [26] J. Wiehe, J. Thiele, A. Walter, A. Hashemifarzad, J. Hingst, C. Haaren, Nothing to regret: Reconciling renewable energies with human wellbeing and nature in the German Energy Transition, *International Journal of Energy Research* 45 (2021) 745–758. URL: <https://onlinelibrary.wiley.com/doi/10.1002/er.5870>. doi:10.1002/er.5870.
- [27] [dataset] European Commission. Joint Research Centre., The European settlement map 2017 release: methodology and output of the European settlement map (ESM2p5m). (2016). URL: <https://data.europa.eu/doi/10.2760/780799>. doi:10.2760/780799.
- [28] R. McKenna, S. Hollnacher, W. Fichtner, Cost-potential curves for onshore wind energy: A high-resolution analysis for Germany, *Applied Energy* 115 (2014) 103–115. URL: <https://linkinghub.elsevier.com/retrieve/pii/S0306261913008507>. doi:10.1016/j.apenergy.2013.10.030.
- [29] F. Sensfuß, K. Franke, D. C. Kleinschmitt, Langfrist-szenarien 3 - Potentiale Windenergie an Land - Datensatz

- 174, Technical Report, Bundesministerium für Wirtschaft und Energie (BMWi), Karlsruhe, 2021. URL: <https://www.langfristszenarien.de/enertile-explorer-wAssets/docs/Potentiale-Windenergie-an-Land-Datensatz-174-final.pdf>.
- [30] [dataset] Eurostat, EuroStat Urban 2011 (2011). URL: <https://ec.europa.eu/eurostat/web/gisco/geodata/reference-data/population-distribution-demography/clusters>.
- [31] [dataset] G. ©. G.-D. . B. (2012), Digitales Landschaftsmodell 1:250 000 (Ebenen) (DLM250) (2012).
- [32] Fachagentur Wind an Land, Entwicklung der Windenergie im Wald, 2021.
- [33] Fachagentur Wind an Land, Überblick Abstandsempfehlungen und Vorgaben zur Ausweisung von Windenergiegebieten in den Bundesländern, 2021.
- [34] Baugesetzbuch in der Fassung der Bekanntmachung vom 3. November 2017 (BGBl. I S. 3634), das zuletzt durch Artikel 9 des Gesetzes vom 10. September 2021 (BGBl. I S. 4147) geändert worden ist, 2017.
- [35] [dataset] Geobasisdaten: © GeoBasis-DE / BKG (2021), Amtliche Hausumringe Deutschland (HU-DE) (2021).
- [36] D. S. Ryberg, D. G. Caglayan, S. Schmitt, J. Linßen, D. Stolten, The Future of European Onshore Wind Energy Potential: Detailed Distribution and Simulation of Advanced Turbine Designs (2018) 22.
- [37] [dataset] Technical University of Denmark, Global Wind Atlas (GWA) 3.0 (2021). URL: <https://globalwindatlas.info/download/gis-files>.
- [38] F. Sensfuß, B. Lux, B. Bernath, Christiane, C. Kiefer, B. Pfluger, C. Kleinschmitt, K. Franke, G. Deac, Langfristszenarien für die Transformation des Energiesystems in Deutschland, Technical Report, Bundesministerium für Wirtschaft und Energie (BMWi), Berlin, 2021. URL: https://www.langfristszenarien.de/enertile-explorer-wAssets/docs/LFS_Kurzbericht_final_v5.pdf.
- [39] J. Bosch, I. Staffell, A. D. Hawkes, Temporally explicit and spatially resolved global offshore wind energy potentials, Energy 163 (2018) 766–781. URL: <https://linkinghub.elsevier.com/retrieve/pii/S036054421831689X>. doi:10.1016/j.energy.2018.08.153.
- [40] W. Zappa, M. van den Broek, Analysing the potential of integrating wind and solar power in Europe using spatial optimisation under various scenarios, Renewable and Sustainable Energy Reviews 94 (2018) 1192–1216. URL: <https://linkinghub.elsevier.com/retrieve/pii/S1364032118304362>. doi:10.1016/j.rser.2018.05.071.
- [41] D. G. Caglayan, D. S. Ryberg, H. Heinrichs, J. Linßen, D. Stolten, M. Robinus, The techno-economic potential of offshore wind energy with optimized future turbine designs in Europe, Applied Energy 255 (2019) 113794. URL: <https://linkinghub.elsevier.com/retrieve/pii/S0306261919314813>. doi:10.1016/j.apenergy.2019.113794.
- [42] D. F. Sensfuß, K. Franke, D. C. Kleinschmitt, Langfristszenarien 3 - Potentiale Windenergie auf See - Datensatz 127, Technical Report, Bundesministerium für Wirtschaft und Energie (BMWi), Karlsruhe, 2021. URL: <https://www.langfristszenarien.de/enertile-explorer-wAssets/docs/Potentiale-der-Windenergie-auf-See-Datensatz-127.pdf>.
- [43] [dataset] 4C Offshore, Global Offshore Renewable Map (2021). URL: <https://map.4coffshore.com/offshorewind/>.
- [44] Bundesamt für Seeschifffahrt und Hydrographie, Entwurf Flächenentwicklungsplan 2020 für die deutsche Nord- und Ostsee, 2020. URL: https://www.bsh.de/DE/THEMEN/Offshore/Meeresfachplanung/Fortschreibung/_Anlagen/Downloads/Entwurf_FEP_2020.pdf;jsessionid=4E1EA7F377C9600D693C60CD059E972B.live11311?__blob=publicationFile&v=6.
- [45] Directorate-General for Maritime Affairs and Fisheries, European Marine Observation and Data Network (EMODnet), 2021. URL: <https://emodnet.ec.europa.eu/en>.
- [46] [dataset] B. Halpern, M. Frazier, J. Potapenko, K. Casey, K. Koenig, C. Longo, J. Lowndes, C. Rockwood, E. Selig, K. Selkoe, S. Walbridge, Cumulative human impacts: raw stressor data (2008 and 2013) (2015). URL: <https://knb.ecoinformatics.org/view/doi:10.5063/F1S180FS>. doi:10.5063/F1S180FS.
- [47] Bundesamt für Seeschifffahrt und Hydrographie, Bundesfachplan Offshore für die deutsche ausschließliche Wirtschaftszone der Nordsee 2016/2017 und Umweltbericht, 2017. URL: https://www.bsh.de/DE/PUBLIKATIONEN/_Anlagen/Downloads/Offshore/Bundesfachplan-Nordsee/Bundesfachplan-Offshore-Nordsee-2016-2017.pdf;jsessionid=4C07B4A5A082CF03C0C83DAB77F4CC16.live21304?__blob=publicationFile&v=15.
- [48] Bundesamt für Seeschifffahrt und Hydrographie, Bundesfachplan Offshore für die deutsche ausschließliche Wirtschaftszone der Ostsee 2016/2017 und Umweltbericht, 2017.
- [49] [dataset] Bundesamt für Seeschifffahrt und Hydrographie, Raumordnungsplan AWZ – WMS (2021). URL: <https://www.geoseaportal.de/mapapps/resources/apps/meeresnutzung/index.html?lang=de>.
- [50] [dataset] Niedersächsisches Ministerium für Ernährung, Landwirtschaft und Verbraucherschutz, Neubekanntmachung der LROP-Verordnung 2017 (2017). URL: https://www.ml.niedersachsen.de/startseite/themen/raumordnung_landesplanung/landesraumordnungsprogramm/datenabgabe_lrop_2017/neubekanntmachung-der-lrop-verordnung-2017-158625.html.
- [51] [dataset] Ministerium für Energie, Infrastruktur und Digitalisierung, Landesraumentwicklungsprogramm Mecklenburg-Vorpommern 2016 (LEP M-V 2016) (2016). URL: <https://www.regierung-mv.de/Landesregierung/em/Raumordnung/Landesraumentwicklungsprogramm/aktuelles-Programm/>.
- [52] [dataset] Landesplanung Schleswig-Holstein/MILIG, Fortschreibung des Landesentwicklungsplans Schleswig-Holstein 2010 (2. Entwurf 2020) (2021). URL: <https://www.bolapla-sh.de/verfahren/bf4796a7-f729-11ea-a85e-0050569710bc/public/detail#procedureDetailsDocumentlist>.
- [53] [dataset] Bundesamt für Seeschifffahrt und Hydrographie, CONTIS Facilities (2020). URL: https://gdiwiki.bsh.de/wiki/index.php/CONTIS_Facilities.
- [54] [dataset] Bundesamt für Seeschifffahrt und Hydrographie, CONTIS Administration - WMS (2019). URL: https://www.geoseaportal.de/wss/service/CONTIS_Administration/guest?SERVICE=WMS&REQUEST=GetCapabilities&VERSION=1.3.0.
- [55] Bundesamt für Seeschifffahrt und Hydrographie, Flächenentwicklungsplan 2020 für die deutsche Nord- und Ostsee, 2020.
- [56] [dataset] Landesbetrieb Geoinformation und Vermessung (LGV) Hamburg, Flächennutzungsplan Hamburg (2021).
- [57] B. Lux, D. F. Sensfuß, D. G. Deac, D. C. Kiefer, C. Bernath, D. J. Fragoso-Garcia, D. B. Pfluger, Langfristszenarien für die Transformation des Energiesystems in Deutschland - Angebotsseite Treibhausgasneutrale Szenarien, Technical Report, Bundesministerium für Wirtschaft und Energie (BMWi), 2021. URL: https://www.langfristszenarien.de/enertile-explorer-wAssets/docs/LFS_Webinar_Angewandte_final.pdf.
- [58] Landesanstalt für Umwelt Baden-Württemberg, Potenzialanalyse der Freiflächen-Photovoltaik, 2018. URL: <https://www.energieatlas-bw.de/sonne/freiflaechen/potenzialanalyse>.
- [59] C. Seidenstücker, Solarkataster NRW - Neues Tool für die Planung von Freiflächen Photovoltaik, 2020.
- [60] D. S. Ryberg, Generation Lulls from the Future Potential of Wind and Solar Energy in Europe, Ph.D. thesis, RWTH Aachen University, 2019.
- [61] [dataset] European Environment Agency, Global land cover - 250m (2016). URL: <https://www.eea.europa.eu/data-and-maps/data/global-land-cover-250m>.
- [62] [dataset] ESA, GlobCover 2009 (2009). URL: http://due.esrin.esa.int/page_globcover.php.
- [63] [dataset] European Environment Agency, Less favoured areas (2012). URL: <https://www.eea.europa.eu/data-and-maps/figures/less-favoured-areas>.
- [64] Gesetz für den Ausbau erneuerbarer Energien (Erneuerbare-Energien-Gesetz - EEG 2021), 2021. URL: https://www.gesetze-im-internet.de/eeg_2014/EEG_2021.pdf.
- [65] Gesetz für den Ausbau erneuerbarer Energien (Erneuerbare-Energien-Gesetz - EEG 2017), 2017. URL: <https://www>.

- gesetze-im-internet.de/eeg_2014/EEG_2017.pdf.
- [66] [dataset] Ackerbauliches Ertragspotenzial der Böden in Deutschland 1:1.000.000. Datenquelle: SQR1000 V1.0 (2013).
- [67] D. H. Wirth, Recent Facts about Photovoltaics in Germany, 2021. URL: <https://www.ise.fraunhofer.de/en/publications/studies/recent-facts-about-pv-in-germany.html>.
- [68] S. Ong, C. Campbell, P. Denholm, R. Margolis, G. Heath, Land-Use Requirements for Solar Power Plants in the United States, Technical Report NREL/TP-6A20-56290, 1086349, 2013. URL: <http://www.osti.gov/servlets/purl/1086349/>. doi:10.2172/1086349.
- [69] SUNTECH, Ultra X Plus - 132 HALF-CELL MONOFACIAL MODULE, 2021. URL: https://www.suntech-power.com/wp-content/uploads/download/product-specification/EN_Ultra_X_Plus_STP670S_D66_Wmh.pdf.
- [70] LG, LG NEON R - LG370 Q1C-A5, 2021. URL: <https://static1.squarespace.com/static/5354537ce4b0e65f5c20d562/t/5b56f6a18a922dbc850387a9/1532425900596/LG+Solar+Datasheet+2018+NeONR+370.pdf>.
- [71] S. Castellanos, D. A. Sunter, D. M. Kammen, Rooftop solar photovoltaic potential in cities: how scalable are assessment approaches?, *Environmental Research Letters* 12 (2017) 125005. URL: <https://iopscience.iop.org/article/10.1088/1748-9326/aa7857>. doi:10.1088/1748-9326/aa7857.
- [72] K. Mainzer, K. Fath, R. McKenna, J. Stengel, W. Fichtner, F. Schultmann, A high-resolution determination of the technical potential for residential-roof-mounted photovoltaic systems in Germany, *Solar Energy* 105 (2014) 715–731. URL: <https://linkinghub.elsevier.com/retrieve/pii/S0038092X14002114>. doi:10.1016/j.solener.2014.04.015.
- [73] K. Mainzer, S. Killinger, R. McKenna, W. Fichtner, Assessment of rooftop photovoltaic potentials at the urban level using publicly available geodata and image recognition techniques, *Solar Energy* 155 (2017) 561–573. URL: <https://linkinghub.elsevier.com/retrieve/pii/S0038092X17305686>. doi:10.1016/j.solener.2017.06.065.
- [74] X. Song, Y. Huang, C. Zhao, Y. Liu, Y. Lu, Y. Chang, J. Yang, An Approach for Estimating Solar Photovoltaic Potential Based on Rooftop Retrieval from Remote Sensing Images, *Energies* 11 (2018) 3172. URL: <http://www.mdpi.com/1996-1073/11/11/3172>. doi:10.3390/en11113172.
- [75] A. Sampath, P. Bijapur, A. Karanam, V. Umadevi, M. Parathodiyil, Estimation of rooftop solar energy generation using Satellite Image Segmentation, in: 2019 IEEE 9th International Conference on Advanced Computing (IACC), IEEE, Tiruchirappalli, India, 2019, pp. 38–44. URL: <https://ieeexplore.ieee.org/document/8971578/>. doi:10.1109/IACC48062.2019.8971578.
- [76] R. Singh, R. Banerjee, Estimation of roof-top photovoltaic potential using satellite imagery and GIS, in: 2013 IEEE 39th Photovoltaic Specialists Conference (PVSC), IEEE, Tampa, FL, USA, 2013, pp. 2343–2347. URL: <http://ieeexplore.ieee.org/document/6744945/>. doi:10.1109/PVSC.2013.6744945.
- [77] E. Grothues, C. Seidenstücker, Das landesweite Solarkataster Nordrhein-Westfalen, Technical Report 43, Landesamt für Natur, Umwelt und Verbraucherschutz Nordrhein-Westfalen (LANUV), 2018.
- [78] A. Strzalka, N. Alam, E. Duminil, V. Coors, U. Eicker, Large scale integration of photovoltaics in cities, *Applied Energy* 93 (2012) 413–421. URL: <https://linkinghub.elsevier.com/retrieve/pii/S0306261911008294>. doi:10.1016/j.apenergy.2011.12.033.
- [79] A. Walch, R. Castello, N. Mohajeri, J.-L. Scartezzini, Big data mining for the estimation of hourly rooftop photovoltaic potential and its uncertainty, *Applied Energy* 262 (2020) 114404. URL: <https://linkinghub.elsevier.com/retrieve/pii/S0306261919320914>. doi:10.1016/j.apenergy.2019.114404.
- [80] K. Fath, J. Stengel, W. Sprenger, H. R. Wilson, F. Schultmann, T. E. Kuhn, A method for predicting the economic potential of (building-integrated) photovoltaics in urban areas based on hourly Radiance simulations, *Solar Energy* 116 (2015) 357–370. URL: <https://linkinghub.elsevier.com/retrieve/pii/S0038092X15001413>. doi:10.1016/j.solener.2015.03.023.
- [81] J. A. Jakubiec, C. F. Reinhart, A method for predicting city-wide electricity gains from photovoltaic panels based on LiDAR and GIS data combined with hourly Daysim simulations, *Solar Energy* 93 (2013) 127–143. URL: <https://linkinghub.elsevier.com/retrieve/pii/S0038092X13001291>. doi:10.1016/j.solener.2013.03.022.
- [82] L. Kurdgelashvili, J. Li, C.-H. Shih, B. Attia, Estimating technical potential for rooftop photovoltaics in California, Arizona and New Jersey, *Renewable Energy* 95 (2016) 286–302. URL: <https://linkinghub.elsevier.com/retrieve/pii/S0960148116302890>. doi:10.1016/j.renene.2016.03.105.
- [83] D. Assouline, N. Mohajeri, J.-L. Scartezzini, Quantifying rooftop photovoltaic solar energy potential: A machine learning approach, *Solar Energy* 141 (2017) 278–296. URL: <https://linkinghub.elsevier.com/retrieve/pii/S0038092X16305850>. doi:10.1016/j.solener.2016.11.045.
- [84] K. Bódis, A high-resolution geospatial assessment of the rooftop solar photovoltaic potential in the European Union, *Renewable and Sustainable Energy Reviews* (2019) 13.
- [85] T. Schmid, F. Jetter, T. Limmer, Regionalisierung des Ausbaus der Erneuerbaren Energien - Begleitdokument zum Netzentwicklungsplan Strom 2035 (Version 2021), 2021.
- [86] M. Portmann, D. Galvagno-Erny, P. Lorenz, D. Schacher, R. Heinrich, Sonnendach.ch und Sonnenfassade.ch: Berechnung von Potenzialen in Gemeinden, 2019.
- [87] J.-B. Eggers, M. Behnisch, J. Eisenlohr, H. Poglitsch, W.-F. Phung, C. Ferrara, T. E. Kuhn, PV-Ausbauerfordernisse versus Gebäudepotenzial: Ergebnis einer gebäudescharfen Analyse für ganz Deutschland, 2020, p. 21.
- [88] M. Kaltschmitt, Potentiale und Kosten regenerativer Energieträger in Baden-Württemberg, 1992. URL: [HTTP://zbsfx.zb.kfa-juelich.de/sfx_local?sid=google&auinit=M&aulast=Kaltschmitt&title=Potentiale%20und%20Kosten%20regenerativer%20Energietr%C3%A4ger%20in%20Baden-W%C3%BCrttemberg&genre=book&date=1992](http://zbsfx.zb.kfa-juelich.de/sfx_local?sid=google&auinit=M&aulast=Kaltschmitt&title=Potentiale%20und%20Kosten%20regenerativer%20Energietr%C3%A4ger%20in%20Baden-W%C3%BCrttemberg&genre=book&date=1992).
- [89] International Energy Agency (IEA), Potential for Building Integrated Photovoltaics, 2002.
- [90] F. Biljecki, H. Ledoux, J. Stoter, An improved LOD specification for 3D building models, *Computers, Environment and Urban Systems* 59 (2016) 25–37. URL: <https://linkinghub.elsevier.com/retrieve/pii/S0198971516300436>. doi:10.1016/j.compenurbsys.2016.04.005.
- [91] [dataset] Geobasisdaten: © GeoBasis-DE / BKG (2021), 3D-Gebäudemodelle LoD2 Deutschland (LoD2-DE) (2021).
- [92] Bezirksregierung Köln, Nutzerinformationen zur 3D-Gebäudemodelle-übersicht für NRW, 2021. URL: https://www.bezreg-koeln.nrw.de/brk_internet/geobasis/3d_gebaudemodelle/nutzer_info_3d-gm-uebersicht.pdf.